**Supporting information**

# Synthesis of Wurtzite - Zincblende $Cu_2ZnSnS_4$ and $Cu_2ZnSnSe_4$ Nanocrystals: Insight into the Structural Selection of Quaternary and Ternary Compounds influenced by Binary nucleus

Yingwei Li, Qifeng Han*, Tae Whan Kim and Wangzhou Shi

**Table S1** Samples with various mole ratios. It should be noted that the reagents contained more than stoichiometric amount of zinc salt due to lower reactivity of the Zn source. And for standard samples (Q1 to Q3, T1 to T4, B1 to B4), mole mass of $S^{2-}$ or $Se^{2-}$ was kept excessive to prepare NCs in a moderate S (or Se)-rich ambient. By contrary, for controlled samples (Q5, Q6, B6 and B7), the consumption of $SC(NH_2)_2$ or $SeC(NH_2)_2$ was further increased, resulting in a considerably S (or Se)-rich ambient.

| Sample No. | Compound | mole ratio |  |  |  | Anion source |
|---|---|---|---|---|---|---|
|  |  | Cu | Zn | Sn(Ge) | S(Se) |  |
| Q1 | CZTS | 2 | 1.5 | 1 | 5 | $SC(NH_2)_2$ |
| Q2 | CZTSe |  |  |  |  | $SeC(NH_2)_2$ |
| Q3 | CZGS |  |  |  |  | $SC(NH_2)_2$ |
| Q4 | CZTSe-WZ enhanced |  |  |  | 4 | $SeC(NH_2)_2$ |
| Q5 | CZTSe-ZB enhanced |  |  |  | 6 |  |
| Q6 | CZTS-ZB enhanced |  |  |  |  | $SC(NH_2)_2$ |
| T1 | CTS | 2 | 0 | 1 | 4 | $SC(NH_2)_2$ |
| T2 |  |  |  |  |  | S powder |
| T3 | CTSe |  |  |  |  | $SeC(NH_2)_2$ |
| T4 |  |  |  |  |  | $(C_6H_5)_2Se_2$ |
| B1 | Cu-S | 2 | 0 | 0 | 3 | $SC(NH_2)_2$ |
| B2 |  |  |  |  |  | S powder |
| B3 | Cu-Se |  |  |  |  | $SeC(NH_2)_2$ |
| B4 |  |  |  |  |  | $(C_6H_5)_2Se_2$ |
| B5 | Cu-Se-$Cu_2Se$ enhanced |  |  |  | 1 | $SeC(NH_2)_2$ |
| B6 | Cu-Se-CuSe enhanced |  |  |  | 4 |  |
| B7 | Cu-S-CuS enhanced |  |  |  |  | $SC(NH_2)_2$ |
| B8 | ZnS | 0 | 1.5 | 0 | 3 | $SC(NH_2)_2$ |
| B9 | ZnSe |  |  |  |  | $SeC(NH_2)_2$ |

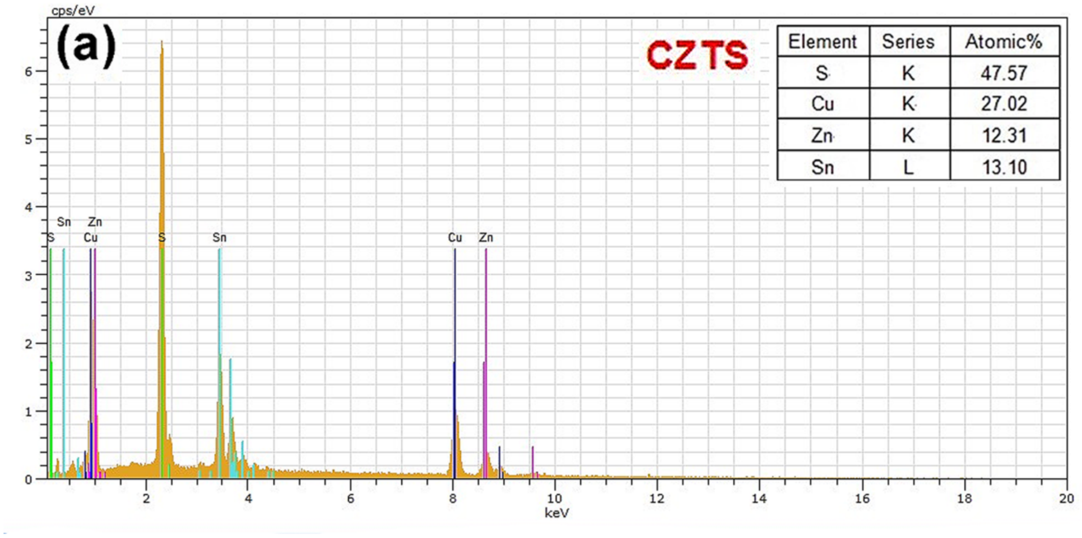

| Element | Series | Atomic% |
|---|---|---|
| S | K | 47.57 |
| Cu | K | 27.02 |
| Zn | K | 12.31 |
| Sn | L | 13.10 |

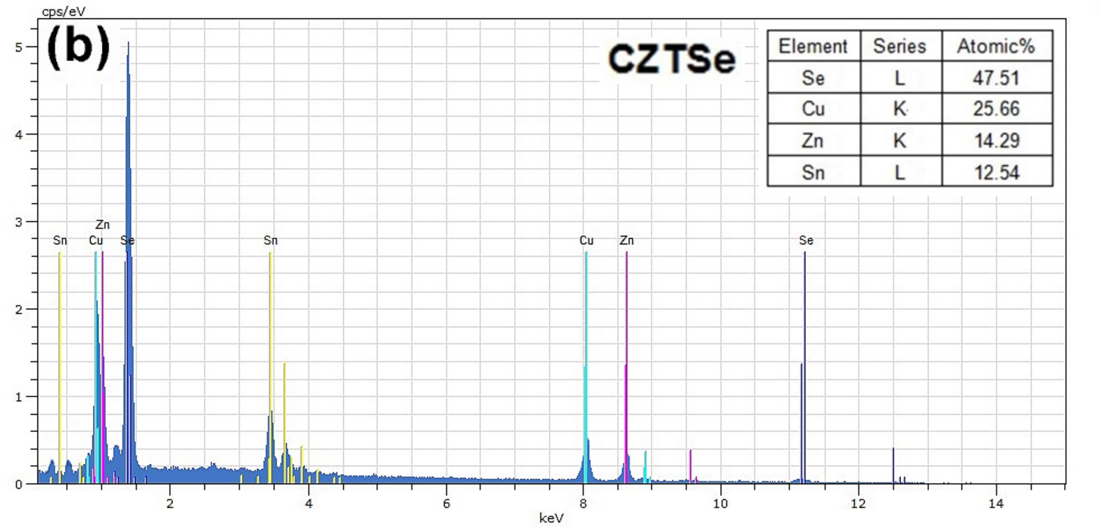

| Element | Series | Atomic% |
|---|---|---|
| Se | L | 47.51 |
| Cu | K | 25.66 |
| Zn | K | 14.29 |
| Sn | L | 12.54 |

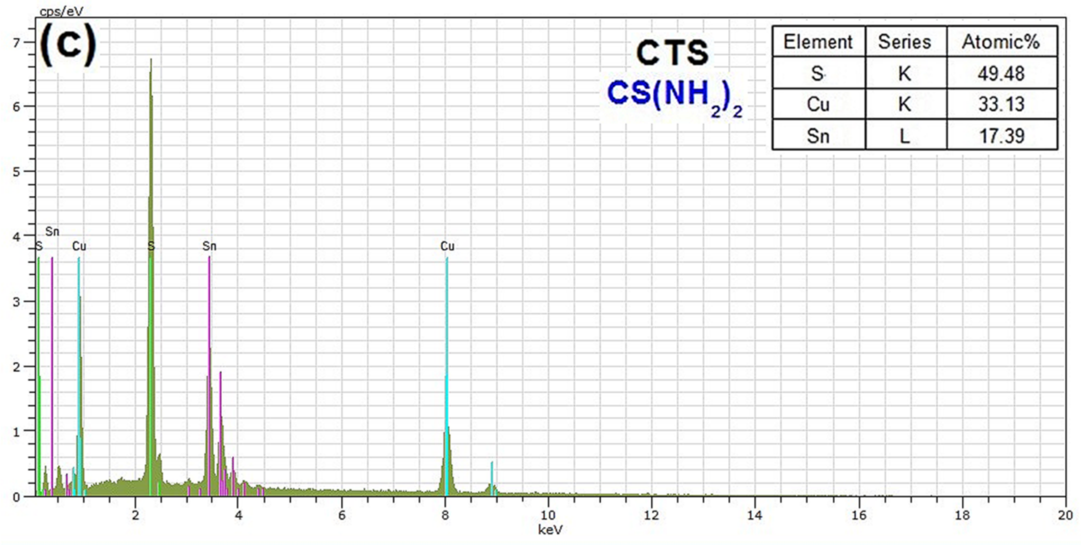

| Element | Series | Atomic% |
|---|---|---|
| S | K | 49.48 |
| Cu | K | 33.13 |
| Sn | L | 17.39 |

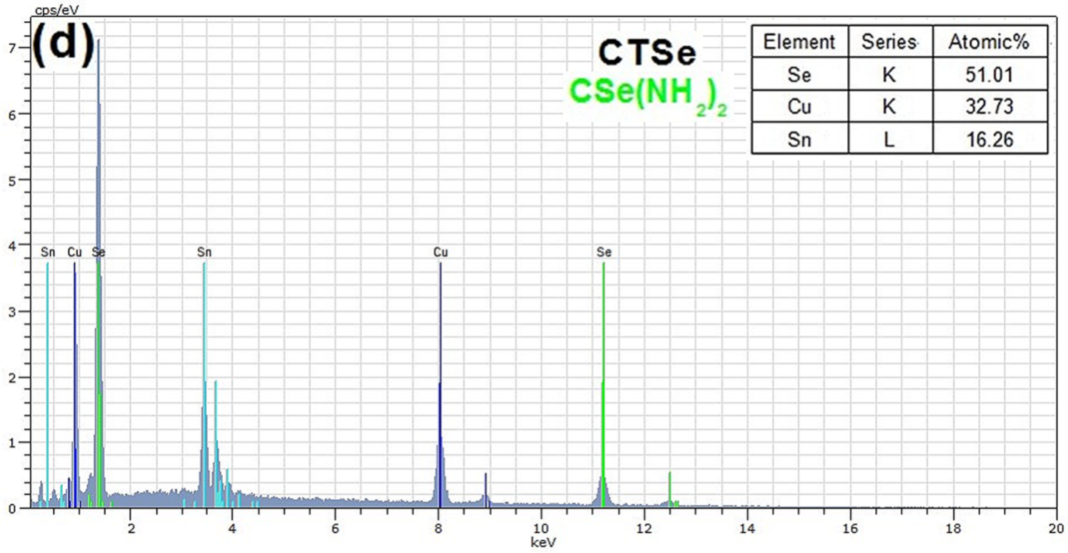

**Figure S1** EDS results for (a) CZTS, (b) CZTSe, (c) CTS, and (d) CTSe NCs prepared with $SC(NH_2)_2$ or $SeC(NH_2)_2$. Figure S1 (a), (b) suggest the near stoichiometric compositions of the quaternary NCs in which CZTSe NCs are Cu-poor and Zn-rich, more satisfactory for solar cell application. Figure S1 (c), (d) also demonstrate the formation of $Cu_2SnS_3$ and $Cu_2SnSe_3$ NCs.

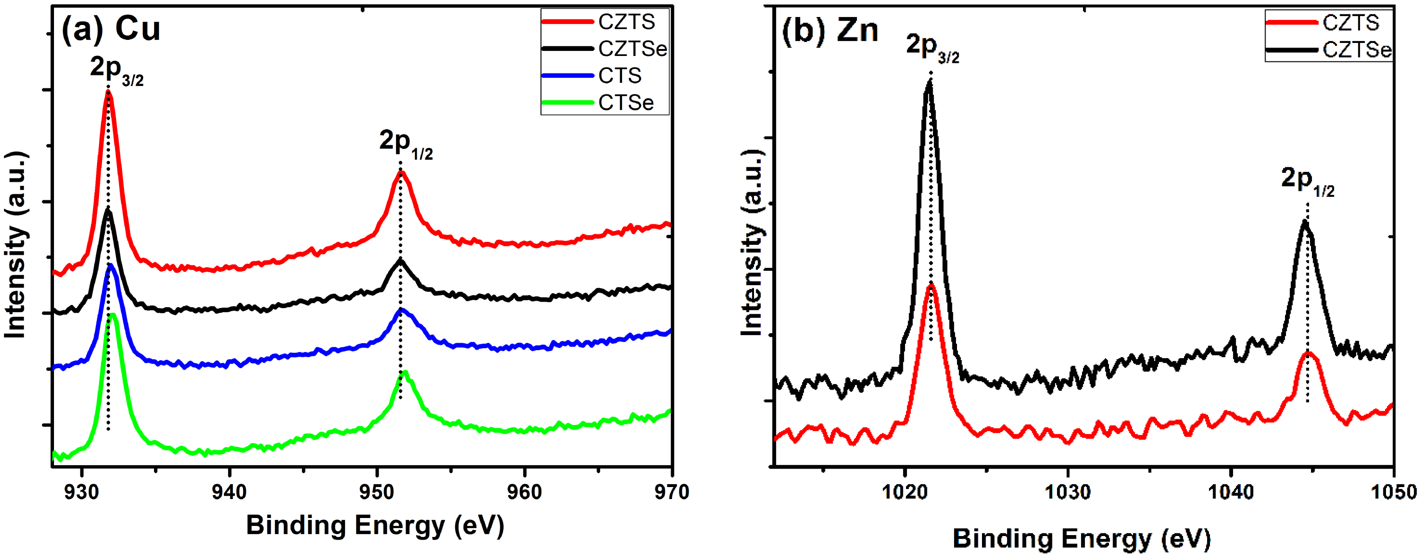

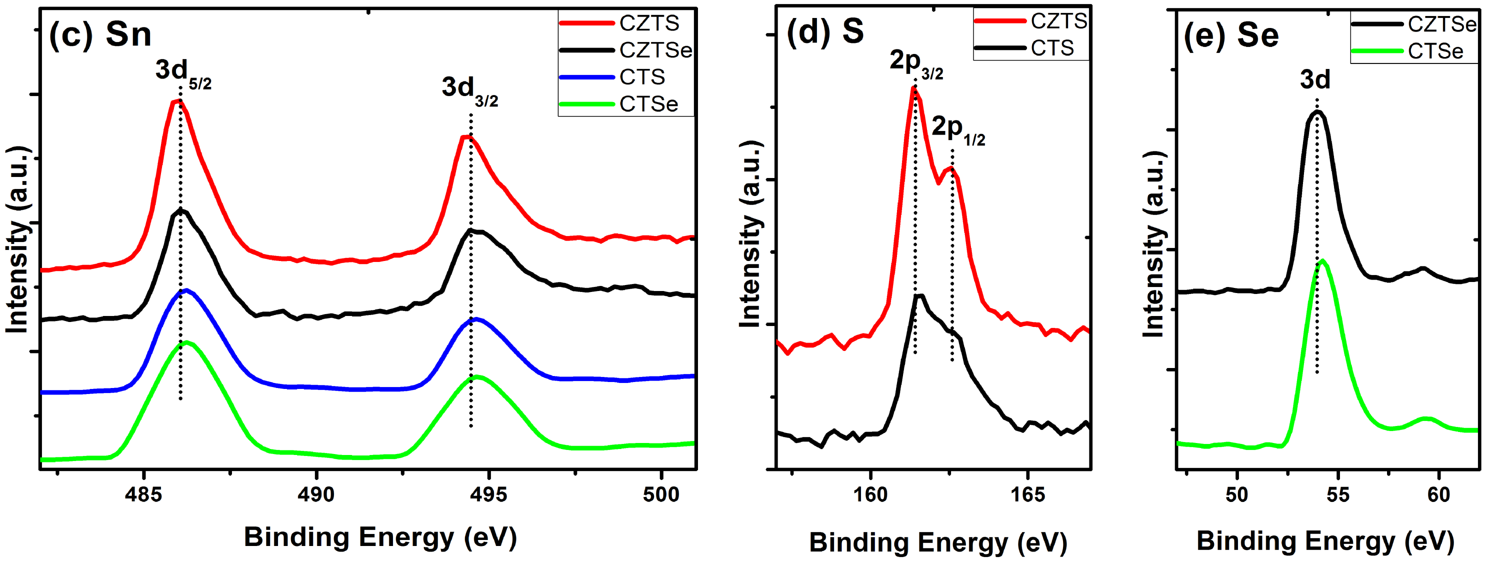

**Figure S2** XPS analyses of the five elements in CZTS, CZTSe, CTS and CTSe NCs.

For all the samples, the copper XPS spectra show two symmetric peaks at 931.8 eV ($2p_{3/2}$) and 951.6 eV ($2p_{1/2}$) with a peak splitting of 19.8 eV which is in good accordance with the value of Cu(I). Peaks of Zn 2p split into 1021.4 eV ($2p_{3/2}$) and 1044.6 eV ($2p_{1/2}$), indicative of Zn(II) with a standard peak splitting of 23 eV. The binding energy (BE) of Sn $3d_{5/2}$ and $3d_{3/2}$ locate at 485.9 eV and 494.3 eV respectively, and the split orbit of 8.4 eV can be assigned to Sn(IV). In Figure S2 (d), sulfur represents its $2p_{3/2}$ and $2p_{1/2}$ peaks at 161.4 eV and 162.6 eV, the energy difference of which is consistent with the 160-164 eV range of S in the sulfide phases. Finally, the BE of Se 3d core levels is located at 53.9 eV (Figure S2 (e)). From the whole XPS results, other valences such as Cu(II) and Sn(II) cannot be detected and it is not probably that $Cu_3SnS_4$ or $Cu_3SnSe_4$ coexists.

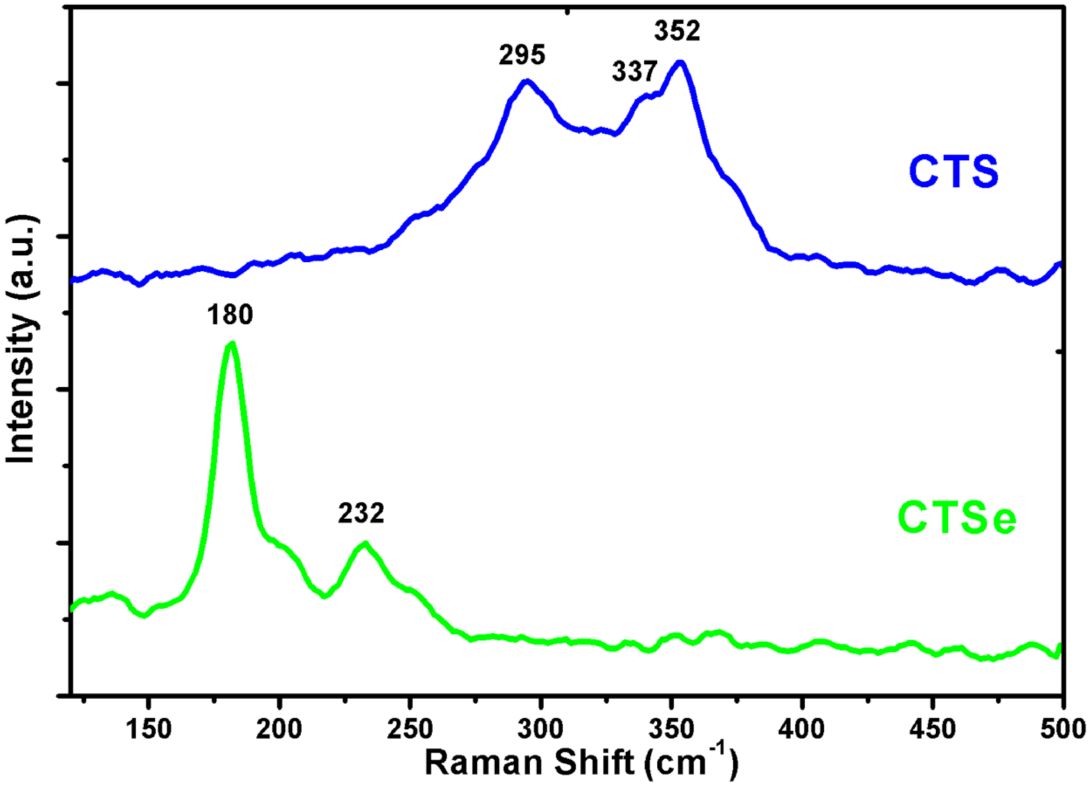

**Figure S3** Raman analysis for CTS and CTSe NCs.

**Table S2** Crystal structures of ternary and quaternary NCs. Some data are collected from other references. By now, we conclude that the S or Se sources have a determinative influence on what kind of structure CTS (or CTSe) and CZTS (or CZTSe) NCs will form.

| **Anion source** | **Ligand/solvent** | **Compound** | **Crystal structure** |
|---|---|---|---|
| $SC(NH_2)_2$ | Oleylamine | $Cu_2SnS_3$<br>$Cu_2ZnSnS_4$ | Wurtzite-dominant<br>+ Zincblende |
| S powder | | $Cu_2SnS_3$<br>$Cu_2ZnSnS_4$ (Ref. 3-5,32-34) | Zincblende |
| $SeC(NH_2)_2$ | | $Cu_2SnSe_3$<br>$Cu_2ZnSnSe_4$ | Zincblende-dominant<br>+ Wurtzite |
| $(C_6H_5)_2Se_2$ | | $Cu_2SnSe_3$<br>$Cu_2ZnSnSe_4$ (Ref. 9,20) | Wurtzite |
| DDT | | $Cu_2SnS_3$ (Ref. 10)<br>$Cu_2ZnSnS_4$ (Ref. 10, 19, 20) | Wurtzite |

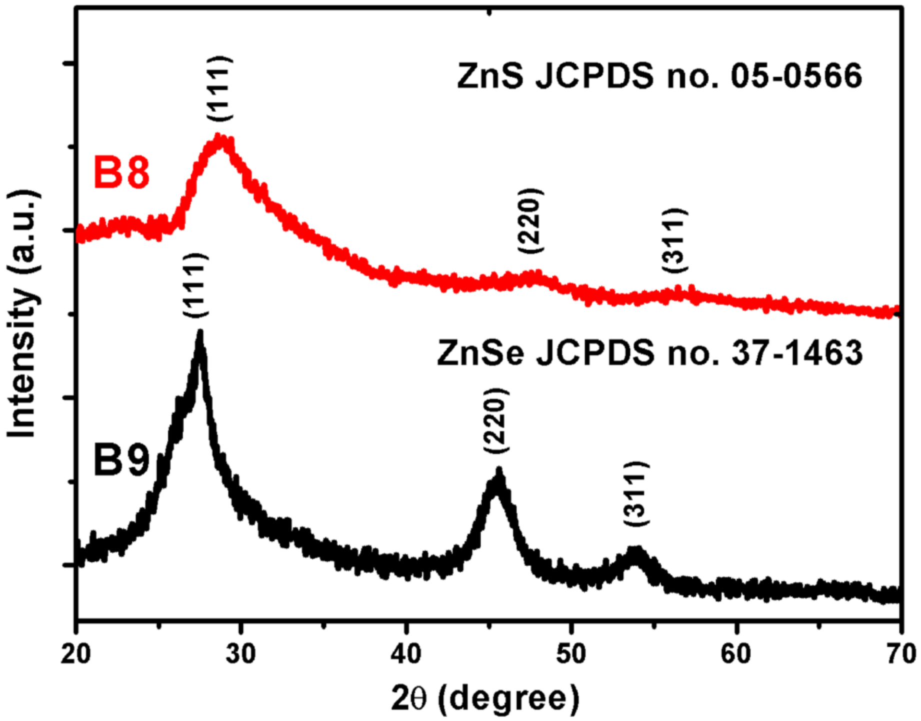

**Figure S4** XRD of ZnS and ZnSe nanocrystals.

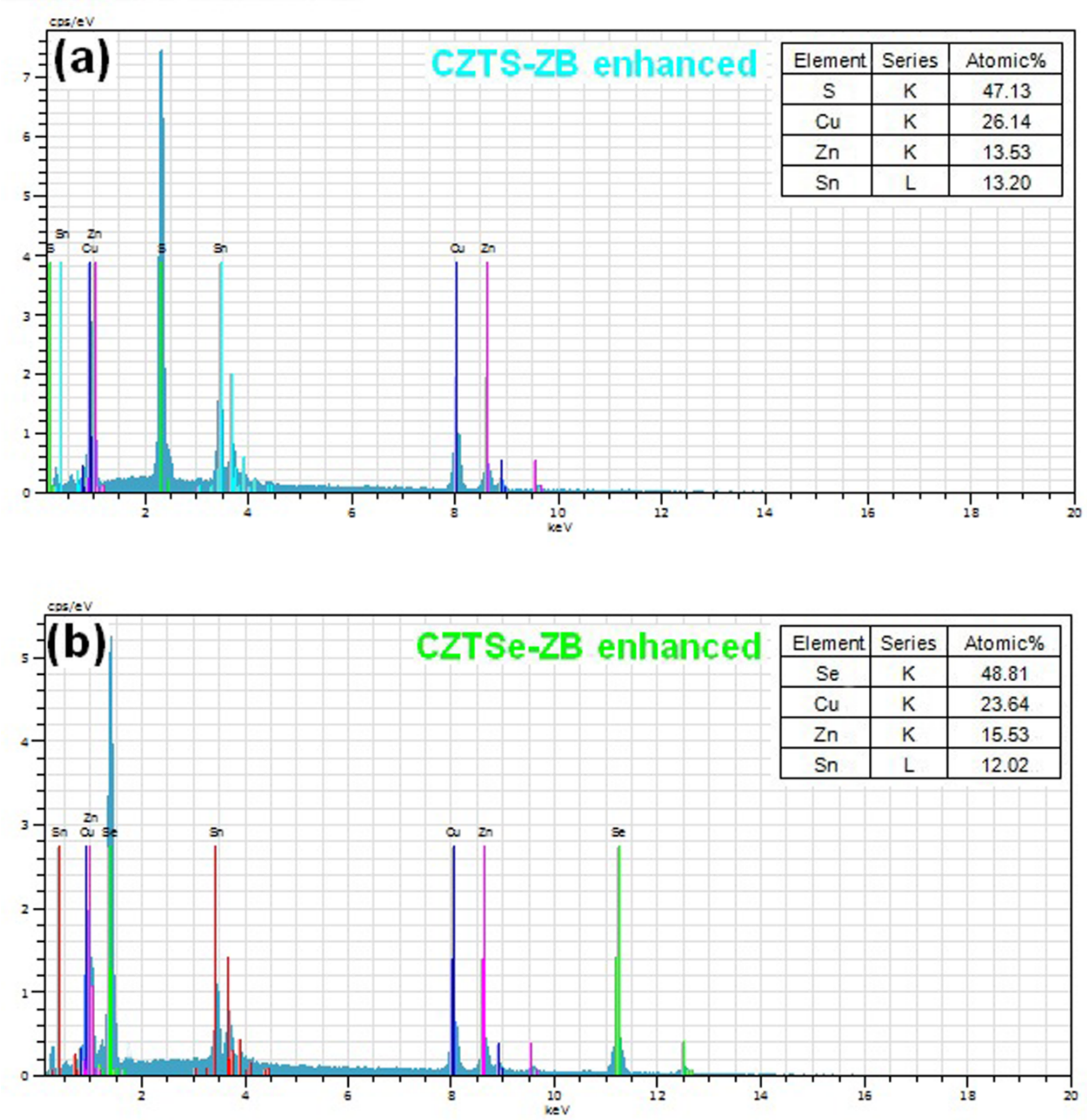

| Element | Series | Atomic% |
|---|---|---|
| S | K | 47.13 |
| Cu | K | 26.14 |
| Zn | K | 13.53 |
| Sn | L | 13.20 |

| Element | Series | Atomic% |
|---|---|---|
| Se | K | 48.81 |
| Cu | K | 23.64 |
| Zn | K | 15.53 |
| Sn | L | 12.02 |

**Figure S5** EDS results for (a) CZTS-ZB enhanced (Q6), and (b) CZTSe-ZB enhanced (Q5). EDS indicates CZTS and CZTSe NCs can be obtained under considerably $S^{2-}$ or $Se^{2-}$ rich conditions. ZB enhanced CZTS NCs (Q6) become slightly Cu-poor and Zn-rich. Composition of ZB enhanced CZTSe NCs (Q5) deviates from stoichiometry, but Cu-poor and Zn-rich composition is desirable for high efficiency solar cells.